MATHEMATICAL MODELING OF A PHOTOCHEMICAL FILM REACTOR

Krishna Gopal Singh[+]*, Sandeep Mourya, and Ashok N. Bhaskarwar*[*]
Department of Chemical Engineering
Indian Institute of Technology
Hauz Khas, New Delhi-110016, INDIA.

ABSTRACT

The design, operation, and performance of a photochemical parallel film reactor is analyzed in a comprehensive manner. The reactor consists of many parallel tubes, each having a number of parallel films. These films are separated by uniform gas pockets containing the diffusing reactive gas, which move upwards axially. This part of the reactor is termed as film section. The pool of liquid at the bottom of the reactor from which the films are generated is called as storage section. The general model of the photochemical film reactor developed here is the most rigorous analysis presented so far. Mechanisms and rates of the gas liquid reaction are considered for dark as well as photochemical reaction.

To study the overall performance of the reactor in the comparative sense, the results have been compared with those of a bubble column with the same volume of liquid phase reactant. It has been found that if light intensity is high very small fraction of liquid in film section can give very high reaction rate. It has been observed that when liquid feed is free of gaseous reactant reaction rate is highest in the semi batch mode (batch with respect to liquid). I has also been seen that increasing the height of the film section overall rate increases upto an extent after which it saturates to a fixed limit. Thus, a further increase in the height of the film section would offer no further benefit beyond a certain critical height.

[*] Author to whom all correspondence should be addressed.
E-mail: ashoknb@chemical.iitd.ernet .in;
Phone: 0091-11-26596161; Fax: 0091-11-26581120

[+] Graduate Student
E-mail: kgsingh_99@yahoo.com

INTRODUCTION

There are a number of photochemical reactions, which involve a gas-phase reactant and a liquid-phase reactant. These reactions have considerable practical value in organic synthesis and in treatment of wastewater. Some typical examples are chlorination of n-alkanes and alkyl aromatics, sulfochlorination and sulfoxidation of n-alkanes, nitrosation of cycloalkanes (Fisher, 1978; Prengle et al., 1975). Wastewater treatment includes ozonolysis of wastewater (Schorr et al., 1971) and oxidation of pollutants like azo dyes (Zhao et al, 2005). In such reactions, the gas dissolves and diffuses into the liquid and its reaction with the liquid-phase reactant is enhanced by photons through excitation of either the liquid-phase reactant or of the dissolved gas. If the enhancement is high, the reaction would be confined to the vicinity of the interface. Mahajani and Sharma (1981) have theoretically analyzed the problem of gas absorption with a fast pseudo-first order reaction. They assumed photon absorption by liquid-phase reactant as an irreversible process, and hence photochemical rate to be independent of dissolved gas-phase component's concentration. But if the excited state is unstable (which will be the case in most of the situations) and if the reverse reaction is very fast, then the photochemical-reaction rate will be dependent on the concentration of the dissolved gas-phase reactant.

In such a situation, it would be advantageous to have a reactor where a thin layer of liquid is brought in contact with the gas while passing through an irradiated zone. Foam-bed reactors can provide such thin liquid layers and high interfacial areas. Though foam gives large interfacial area and a reasonable mass-transfer coefficient, there is the problem of poor irradiation because of the complex polyhedral shapes of foam bubbles. Bhaskarwar and Kumar (1991) gave an experimental solution to this problem by proposing a novel configuration of a parallel-film photochemical reactor. According to them this problem can be overcome by passing the foam through a tube whose diameter is comparable to or smaller than the size of the foam bubbles. In these conditions of size restriction the, foam transforms itself into thin liquid films which are perpendicular to the tube axis, and are separated by gas pockets. Illumination of such a film reactor should present no difficulty at all.

An effort is made here to mathematically model such a reactor in detail. The reactions considered in the model are

$$B_{(l)} + h\nu \longrightarrow B^*_{(l)} \text{ (activated)} \qquad (1)$$

$$A_{(g)} + bB_{(l)} \longrightarrow \text{Products} \qquad (2)$$

$$A_{(g)} + bB^*_{(l)} \longrightarrow \text{Products} \qquad (3)$$

Component *B* that is present in the liquid phase is activated with absorption of a photon (Reaction 1). When gas *A* diffuses into the liquid, it may simultaneously react with reactant *B* (Reaction 2) or with activated *B* (Reaction 3) giving rise to dark and light reactions, respectively.

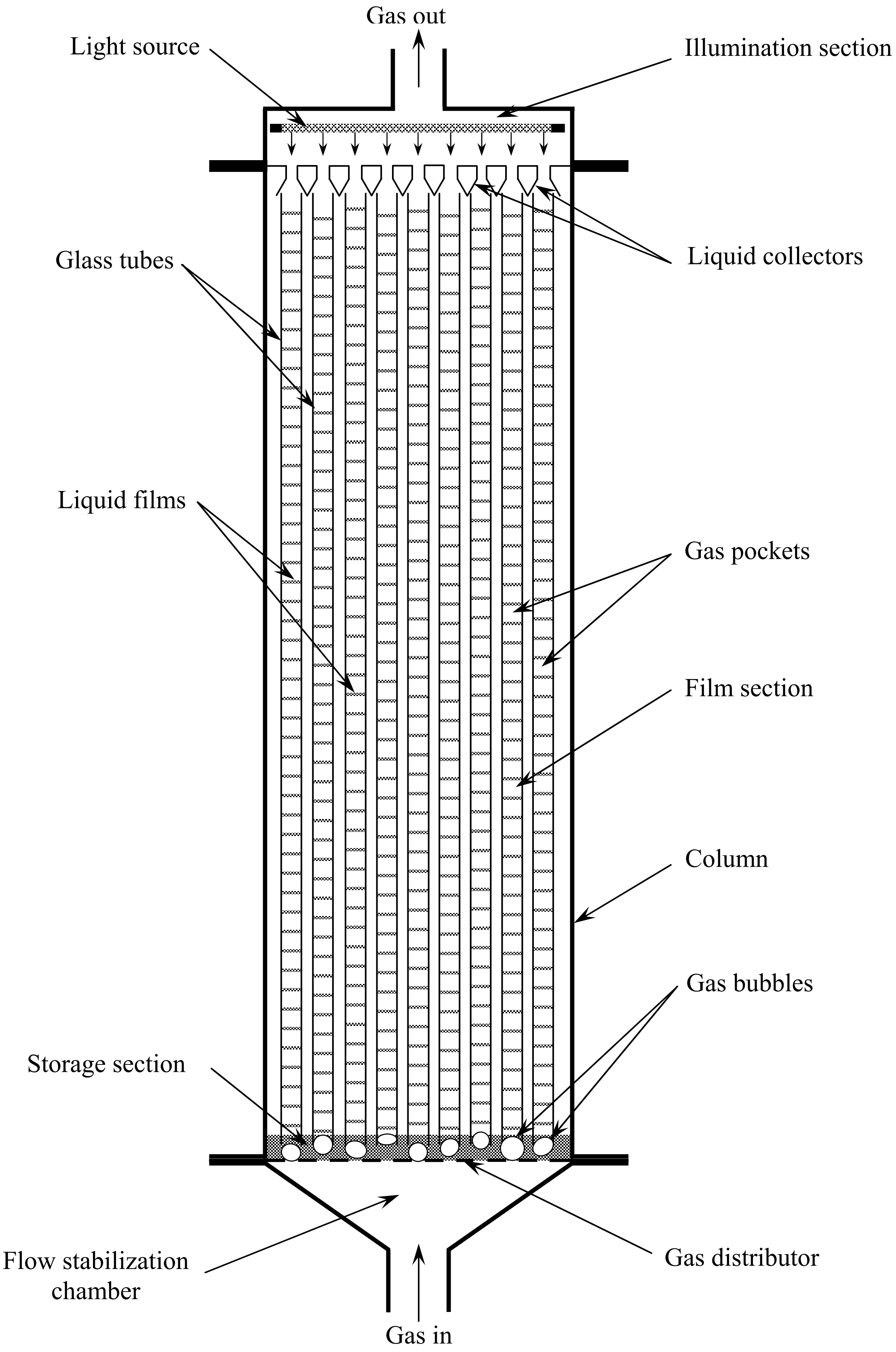

Figure 1: Photochemical film reactor

Description of the photochemical reactor

Figure 1 shows an axially irradiated moving multiple-film reactor (Bhaskarwar and Kumar, 1991). It consists of many parallel tubes, each having a number of parallel liquid films. These films are separated by uniform gas pockets, containing the diffusing reactive gas *A*, which move upwards axially. This part of the reactor is termed as film section. The pool of liquid at the bottom of the reactor from which the films are generated is called as storage section. At the top of the tubes, the films are ruptured and the liquid thus collected is returned to the storage section. During the time of residence of the films in the film section, gas *A* diffuses into the films and reacts there both by the dark-reaction kinetics as well as by the photochemical kinetics. The collimated monochromatic light supplied at the top excites the liquid-phase reactant *B* on being absorbed, and provides the photochemical path. As the liquid film move up towards the source of radiation, they experience an increasing intensity of light. All the tubes are identical and act in parallel. To analyse the extent of gas absorption in the film section, it is therefore sufficient to model what happens in just one of the tubes. In their analysis' Bhaskarwar and Kumar (1991) investigated just the film section of the reactor and assumed that the liquid coming back to the storage section contained no dissolved free *A* and hence did not explore the role of storage section or the overall performance of the photochemical-film reactor. In this paper the possibility of the liquid returning from the film section containing free dissolved *A* has been allowed for. This information can be incorporated into the material-balance equations written over the storage section to obtain a complete quantitative description of the overall performance of the reactor. Bhaskarwar et al. (1991) have done such an analysis for a foam-bed reactor for ordinary gas-liquid reactions. Here, we have used a similar approach to extend the analysis to photochemical gas-liquid reaction systems in a parallel film photo reactor.

Description of the various processes

The various physical and chemical events occurring within a photochemical-film reactor may be summarized as follows:

1. The formation and rise of gas bubbles in the storage section, and diffusion-cum-reaction of the gas-phase reactive component *A*, during the time of residence of the bubbles, in the liquid in storage section.
2. Continuous ascent of a part of liquid from the storage section into the film section in the form of liquid films. The liquid will have reacting dissolved gas, and the composition of gas entering the film section will be different from that at inlet to the storage section.
3. Diffusion-cum-reaction of the gas-phase reactant *A* from the gas pockets into the liquid in the films. At the end of the contact time in the film section, some dissolved gas may remain unreacted in the liquid films.
4. Continuous drainage of partially reacted liquid, containing dissolved gas, from the film section into the storage section after the rupture of the films at the top of the tubes. The liquid drains down to the storage section without further coming in contact with the gas, once the films are disengaged from the gas pockets.

5. Homogeneous reaction of dissolved unreacted *A* with the reactant solute *B* (and excited solute B^*) in the bulk of the solution in the storage section which is assumed to be well stirred.
6. Continuous flow of liquid containing dissolved reactant *B* across the storage section at a constant rate. It will be zero for a semi-batch mode of operation of the photochemical-film reactor.
7. Transport of radiation from the source fixed at the top of the film section through the moving liquid films and then through the gas-in-liquid dispersion in the storage section. Light gets absorbed in the liquid in the reactor and enhances the overall reaction rate through the photochemical route.

A general and comprehensive analysis of a continuous photochemical-film reactor should consider all these seven-coupled processes. This involves development of sub-models for gas absorption with chemical reactions (dark and photochemical) in the surface elements in the storage section and for the same in the films, and subsequent incorporation of these sub models into the general material balances for the species *A* (gaseous), *A* (liquid phase) and *B* (liquid phase) written over the storage section.

DEVELOPMENT OF THE MODEL

Analysis of the film section

Light intensity in the film section

Light absorption occurs mainly in the liquid films. It is assumed here that only the liquid films absorb the radiation. In actual film reactor, there will be some reflection of light. If *k* is wave number of light, *n* is reflective index of film and if we take refractive index of gas phase as 1 than we define $\tau = (2\sqrt{n})/(n+1)$ and $\rho = (n-1)/(n+1)$. If we consider multiple reflection of light from a film followed by interference then intensity of reflected and transmitted light will be given by

$$\frac{I_t}{I_i} = \frac{\tau^4 e^{-2\alpha C_B \delta_f}}{(1-\rho^2 e^{-\alpha C_B \delta_f}\cos(2k\delta_f))^2 + (\rho^2 e^{-\alpha C_B \delta_f}\sin(2k\delta_f))^2} = T \qquad (4)$$

$$\frac{I_r}{I_i} = \rho^2 \frac{(1-e^{-\alpha C_B \delta_f}\cos(2k\delta_f))^2 + (e^{-\alpha C_B \delta_f}\sin(2k\delta_f))^2}{(1-\rho^2 e^{-\alpha C_B \delta_f}\cos(2k\delta_f))^2 + \rho^2 (e^{-\alpha C_B \delta_f}\sin(2k\delta_f))^2} = R \qquad (5)$$

Using these relations we can develop a pair of linear equation for each film (one for transition and other for reflection) and the these equations can be solved to give transmitted as well as reflected light for each film given that light intensity coming from top of film section and that reflected by storage section is known.

In this paper, we however assume that there is no reflection of light from the films. There is only absorption and transmission of light to a good approximation. Accordingly, the intensity is assumed to vary in a discontinuous way with no attenuation occurring in the gas phase. Thus when the light reaches $(n_f+1)^{th}$ film it would have actually travelled a distance of $n_f(\delta_f+\delta_p)$ if the first film is assumed to be right at the top of the tube. The actual attenuation would however have taken place for a path length of $n_f\delta_f$. The intensity at the interface of $(n_f+1)^{th}$ film from the top is therefore given by

$$I_{on} = I_o.\exp(-a.C_B.n_f.\delta_f) \tag{6}$$

If we do not consider the discontinuity in the light received by the film, then this can be approximated by a new extinction coefficient

$$\alpha' = \alpha.\delta_f/(\delta_f + \delta_p) \tag{7}$$

This expression for α' yields the correct value of α, if the gas pockets are missing as in the limiting case of a homogeneous liquid column. In an actual contactor, there will be both absorption and scattering of radiation. In the present analysis, as stated earlier the attenuation has been assumed to be due to absorption only. Further, any absorption of radiation by the small amount of surfactant used to stabilise the liquid films has been neglected as we are not dealing with reaction in monolayer here. Using this value of α', the light intensity received at the upper interface of any film can be approximated by

$$I_{on} = I_o \exp[-\alpha' C_B(H - u_b t_c)] \tag{8}$$

where $(H\text{-}u_b t_c)$ is the distance of film from the top of the film section and is approximately equal to $n_f(\delta_f+\delta_p)$ for $(n_f+1)^{th}$ film. Using this value of I_{on}, the amount of light absorbed per unit volume in the liquid film is given approximately by

$$I_a = I_o\alpha.C_B.\exp[-\alpha'.C_B(H - u_b.t_c)] \tag{9}$$

The basic repeating unit in the film section of the reactor is a liquid film of uniform thickness surrounded on each side by limited amounts of gas corresponding to half the size of a gas pocket. The liquid film is assumed to be flat having no internal flow. There could be a small section adjacent to the wall where the film thickness would be larger. Further, there will be circulation in this small section. In this model, the film is assumed to be of a uniform thickness without any circulation, because of the very small fraction of the film area to which the above effects are confined. The film along with the surrounding gas pockets moves upward as a plug until it is ruptured at the top. As every unit moves up with the same constant velocity, all units spend an identical time in the film section. The radiation intensity received by the liquid film varies as a function of time. Although there is an intensity variation inside a film as a function of depth from its top surface, we assume in writing equation (10), that the photochemical-reaction rate can be calculated on the basis of an average intensity of light in the film. This average intensity is however allowed to change with time. It is also assumed that the concentration of A in the gas phase is same on both sides of the film. If we accept these two assumptions, then the consequent concentration profile of dissolved gas-phase reactant will be symmetric around the middle of the film. The assumption of symmetry facilitates a significant ease and analytical clarity in the mathematical solution of the problem.

With these assumptions, the equation governing the diffusion of *A*, and its reaction in presence of light, in the liquid film is obtained as

$$\frac{\partial C_{Af}}{\partial t_c} = D_A \frac{\partial^2 C_{Af}}{\partial x^2} - \lambda C_{Af} - \frac{K_2^{'} I_a C_{Af}}{b} \tag{10}$$

where $\lambda = K_2.C_B$ is the pseudo-first order rate constant for the dark reaction assuming the high concentration of *B* to remain substantially constant.

The initial and boundary conditions are as follows

At $t_c = 0;$ $0 \le x < +a;$ $C_{Af} = C_A;$

$x = +a;$ $C_{Af} = K_e C_{AG};$ (i)

At $t_c > 0;$ $x = 0;$ $\frac{\partial C_{Af}}{\partial x} = 0;$ (ii)

$x = +a;$ $-V_P \frac{\partial C_{AG}}{\partial t_c} = D_A.S.\frac{\partial C_{Af}}{\partial x};$ $C_{Af} = K_e.C_{AG}$ (iii)

This partial differential equation (10), subjected to conditions (i)-(iii), is solved by Crank-Nicolson finite-difference implicit method. The total amount of gas absorbed by the liquid film across one interface is given by

$$M_t = S.D_A \int_0^{t_{cf}} \left. \frac{\partial C_{Af}}{\partial x} \right|_{x=+a} dt_c \tag{11}$$

The total amount of gas remaining unreacted in the half film at the time of film rupture is given by

$$M_{fr} = S \int_0^a C_{Af}(x, t_{cf}).dx \tag{12}$$

The amount of A reacted in the half film during time t_{cf} is given by

$$M_r = M_t - M_{fr} + \frac{C_A.V_1}{2} \tag{13}$$

The concentration of unreacted species *A* and *B* in the liquid returned to the storage section is given by

$$C_{AF} = 2.M_{fr} / V_1 \tag{14}$$

and

$$C_{BF} = C_B - 2.b.M_r / V_1 \tag{15}$$

Analysis of the storage section

Light intensity in the storage section

At the bottom of the film section, there is a pool of liquid termed as the storage section across which inlet and outlet ports for liquid are provided. A gas-distributor plate at the bottom of the storage section allows for formation and uniform distrubition of bubbles. Alternatively, an array of nozzles could serve the purpose of gas sparging. The radiation after getting partially screened in the film section reaches the storage section. The intensity of light at the top of the storage section is taken as a weighted average of intensity below the tubes and empty regions between the tubes. Thus intensity at the top of storage section is given obtained as

$$I_o^s = \frac{(\pi R_c^2 - N_t.\pi R_t^2)I_o + N_t.\pi R_t^2 I_o \exp(-\alpha' C_B H)}{\pi R_c^2} \tag{16}$$

In reality, there will be a variation of light intensity inside the storage section because of multiple scattering of light by gas bubbles, especially if the storage section is tall and if there are a number of bubbles rising above each hole in the gas-distributor plate. The multiple scattering is not considered here for a shallow storage wherein the gas-sparging rate is so small as to have only a single bubble rising above each hole in the gas distributor. The intensity of light at the bubble interface at time t after formation of the gas bubble is given by

$$I_o^{'} = I_o^s \exp[-\alpha.C_B(h - u_{bs}.t\ )] \tag{17}$$

Gas hold-up and bubble-swarm velocity in storage section

Terminal velocity of a single bubble in the storage section is calculated using Mendalson’s equation (Equation 18), (Deckwer, 1992). Assuming the storage section to be homogeneous and using Marrucci’s equation (Equation 20), (Marrucci, 1964), the bubble-swarm velocity is calculated by iterating with equations (19) and (20).

$$u_t = \sqrt{\left(\frac{\sigma}{R_b \rho_l} + R_b g\right)} \tag{18}$$

$$\varepsilon = u_g / u_{bs} \tag{19}$$

$$u_{bs} = u_t \frac{(1-\varepsilon)^2}{(1-\varepsilon^{5/3})} \tag{20}$$

Gas absorption accompanied by a photochemical reaction in surface elements

Neglecting the curvature of gas-liquid interface, the mass-balance equation for species *A* diffusing and reacting in a surface element is written as

$$\frac{\partial C_A^{'}}{\partial t_e} = D_A.\frac{\partial^2 C_A^{'}}{\partial x_e^2} - \lambda C_A^{'} - \beta C_A^{'} \tag{21}$$

The associated initial and boundary conditions are as follows,

At $t_e = 0;$ $x_e > 0;$ $C_A^{'} = C_A(\neq 0);$ (iv)

At $t_e \geq 0;$ $x_e = 0;$ $C_A^{'} = C_A^{*} = K_e C_{Ag}$ (v)

At $t_e \geq 0;$ $x_e \to \infty;$ $C_A^{'} = C_A\,\mathrm{e}^{-(\lambda+\beta)t_e}$ (vi)

where

$$\beta = K_2^{'} I_o^{'} \alpha C_B / b$$

Equation (21) has been solved using the Laplace-transform technique to obtain the following concentration profile.

$$C_A^{'} = C_A e^{-(\lambda+\beta)t_e} - C_A e^{-(\lambda+\beta)t_e} erfc(\frac{x_e}{2\sqrt{D_A t_e}}) + \tag{22}$$
$$\frac{C_A^{*}}{2}[e^{-x_e\sqrt{(\lambda+\beta)/D_A}}.erfc(\frac{x_e}{2\sqrt{D_A t_e}} - \sqrt{(\lambda+\beta)t_e}) + e^{x_e\sqrt{(\lambda+\beta)/D_A}}.erfc(\frac{x_e}{2\sqrt{D_A t_e}} + \sqrt{(\lambda+\beta)t_e})]$$

Equation (22) provides the basis of calculation of mass-transfer rates from the gas bubbles ascending through the liquid in storage section.

General Material balance Equations of a Photochemical-film Reactor

The photochemical-film reactor may be idealized within the framework of the following assumptions:

1. The liquid and gas in the storage section are well stirred. This assumption would be adequate for small storage section typical of a photochemical-film reactor.
2. No liquid is lost by evaporation or by entrainment with the exit gas.
3. The dark reaction between the dissolved gas-phase component and the liquid-phase reactant is second order and irreversible. An irreversible photochemical reaction involving excitation of species B accompanies the dark reaction.
4. The scattering of light due to gas bubbles in the storage section is negligible, on account a small population of bubbles in this section.
5. The intensity of light shining on a given surface element remains constant during its lifetime i.e. the diffusion time, td.
6. The gas-liquid interfacial area in the storage section remains constant.
7. In the liquid element, the dark reaction is pseudo-first order with respect to the concentration of A, that of B being virtually constant.
8. The concentration profile of A in the film is symmetric about mid plane.

Based on these assumptions, we can now describe the overall reactor behavior in mathematical terms as follows.

Mass balance for dissolved A in storage section:

$$\begin{aligned} V_L \frac{dC_A}{dt} &= Q_1(C_{Ao} - C_A) + Q_f(C_{AF} - C_A) + \\ &\frac{4\pi R_b^2 N_b}{t_{cd} t_d} \int_0^{t_{cd}} \int_0^{\infty} [C_A^{'} - C_A e^{-(\lambda+\beta)t_e}] \Big|_{t_e = t_d} dx_e dt \\ &\frac{-V_L K_2^{'} I_o^s \alpha C_B C_A}{h} \int_0^h e^{-\alpha C_B l} dl - K_2 C_A C_B V_L \end{aligned} \qquad (23)$$

Mass balance for reactant B in bulk liquid in storage section:

$$\begin{aligned} V_L \frac{dC_B}{dt} &= Q_1(C_{Bo} - C_B) + Q_f(C_{BF} - C_B) - \\ &\frac{4\pi R_b^2 N_b b}{t_{cd} t_d} \int_0^{t_{cd}} [\int_0^{t_d} -D_A \frac{\partial C_A^{'}}{\partial x_e} \Big|_{x_e=0} dt_e - \int_0^{\infty} \{C_A^{'} - C_A e^{-(\lambda+\beta)t_e}\} \Big|_{t_e=t_d} dx_e]dt \\ &\frac{-V_L K_2^{'} I_o^s \alpha C_B C_A b}{h} \int_0^h e^{-\alpha C_B l} dl - bK_2 C_A C_B V_L \end{aligned} \qquad (24)$$

Mass balance for gaseous A in storage section:

$$V^{'} \frac{dC_{Ag}}{dt} = Q_t(C_{Agi} - C_{Ag}) - \frac{4\pi R_b^2 N_b}{t_{cd} t_d} \int_0^{t_{cd}} [\int_0^{t_d} -D_A \frac{\partial C_A^{'}}{\partial x_e} \Big|_{x_e=0} dt_e]dt \qquad (25)$$

The initial conditions for equations (23) to (25) are as follows:

At $t = 0;$ $C_A = C_{Ao}; C_B = C_{Bo}; C_{Ag} = C_{Agi};$ (vii)

where

$$\int_0^{\infty} [C_A^{'} - C_A e^{-(\lambda+\beta)t_e}] \Bigg|_{t_e=t_d} dx_e = C_A^* \sqrt{\frac{D_A}{\lambda+\beta}} erfc(\sqrt{(\lambda+\beta)t_d}) - 2\sqrt{\frac{D_A t_d}{\pi}} C_A e^{-(\lambda+\beta)t_d} \qquad (26)$$

$$\begin{aligned} \int_0^{t_d} -D_A \frac{\partial C_A^{'}}{\partial x_e} \Big|_{x_e=0} dt_e &= \sqrt{\frac{D_A}{\lambda+\beta}} [C_A^* ((\lambda+\beta)t_d erf((\lambda+\beta)t_d) + \\ \sqrt{(\lambda+\beta)t_d} e^{-(\lambda+\beta)t_d} &+ erf(\sqrt{(\lambda+\beta)t_d})/2) - C_A erf(\sqrt{(\lambda+\beta)t_d})] \end{aligned} \qquad (27)$$

Method of Solution

The three equations for the concentration of dissolved A (equation (23)), of liquid-phase reactant B (equation (24)) and of gas-phase A (equation (25)) have been solved numerically, subject to the initial conditions (vii). A fourth-order Runge-Kutta method is used to solve the coupled equations in view of expressions (23)-(25). The contribution of the film section is not considered for the initial time of (tcd+tcf) during which the films only fill up the film section, but do not burst to release any liquid. After this time the contribution of the film section is considered by solving equation (10) with conditions (i)-(iii) using Crank-Nicolson finite-difference scheme.

RESULTS AND DISCUSSION:

The photochemical-film reactor is simulated for properties like of an air-water system with oxygen as gaseous reactant A. The set of parameters chosen are reported in table-1. All other properties are taken for air-water system.

Table-1 List of parameters chosen for simulation (*except where variation of height of film section has been studied)

S.No	Parameter	Value
1	C_{Ao}	0 mol/m^3
2	C_{Bo}	250 mol/m^3
3	C_{Agi}	8.123 mol/m^3
4	K_e	0.03
5	α	1 m^2/mole
6	D_A	2*10^{-9} m^2/s
7	H	0.5 m*
8	δ_f	10^{-4} m
9	Liquid hold-up in film section	0.015
10	N_t	30
11	Total volume of liquid in reactor	10^{-3} m^3
12	Fraction of liquid in the film section	0.017

The results are presented in terms of a transient fractional rate of reaction in film section (Γ) defined as

$$\Gamma = r_f / (r_f + r_s)$$

where r_f is rate in film section and r_s is rate in storage section

In general for any given simulation Γ is zero to begin with and the number of films in the film section increases with time. When the film section becomes filled up with the films the rate of reaction in the film section becomes almost uniform. At the same time, the rate in the storage section increases rapidly because of the unreacted A coming with the liquid drained from the film section. Thus the fractional rate of reaction Γ reaches a maximum and then it decreases. After about 50-60 seconds of reactor start-up, the fractional rate of reaction Γ levels off to a uniform value and it is this value, which is of importance to us.

The overall rate of reaction in a homogeneous bubble column is also computed by setting the height of film section equal to zero in some of the simulations. The ratio of rate of reaction in the film reactor to that in the bubble column (denoted by X) is used as a comparative measure of the relative performance of the two kind's of photoreactors to report the effects of variation of the various system parameters on. Initially, the rate in the photochemical film reactor increases very rapidly when compared to that in the bubble column because of the smaller diffusional length scales and hence the ratio of rates (X) increases very rapidly It passes through a maximum and then levels off after about 50-60 seconds of reactor operation. We shall compare the effects of variation of the rate constants of dark and photochemical reactions and of height of the film section on the ratio of these rates, *X*.

Transient Concentration Profile of Component A in Liquid Film

Figure 2 shows the concentration profile of diffusing gas-phase reactant *A* as it evolves over the time of contact in absence of light and cross flow. The dark-reaction rate constant has been chosen as a parameter, with $K_2 = 10^{-5}$ m^3/(mol.s) and $K_2 = 10^{-4}$ m^3/(mol.s), representing the two reaction velocities. In absence of light, the concentration builds over time in the bulk of the film while it decreases with time at the interface. It can also be seen that the diffusional resistance is larger for faster reaction kinetics.

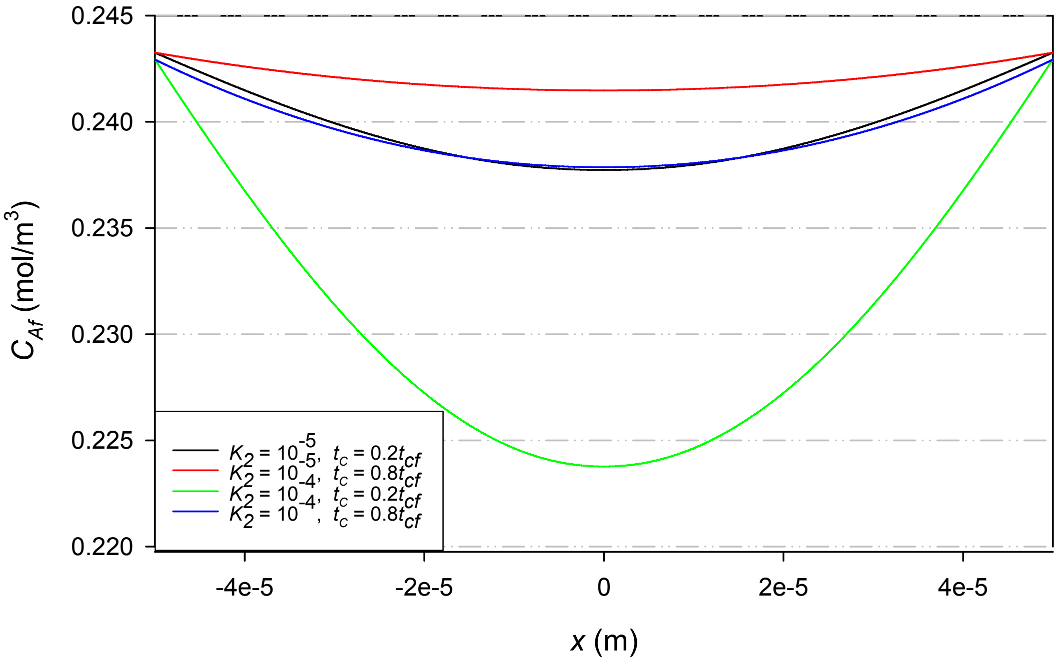

Figure-2, Transient concentration profile in film, Effect of dark reaction constant ($I_O = 0$ E/(m^2/s), $Q_1 = 0$ m^3/s)

Figure 3 shows the concentration profile of the diffusing gas-phase reactant A as it evolves over the time of contact in presence of a light intensity of 10^{-3} E/(m^2.s) ($K_2 = 10^{-5}$ m^3/(mol.s), $Q_1 = 0$ m^3/s). In this case, the concentration builds over time in bulk of the film, reaches a maximum, and then decreases. When the liquid film deficient in *A* is exposed to gas pockets, there are two opposing factors, which govern the concentration in the film. The concentration tends to increase because of diffusion of *A*, and it tends to decrease because of the reaction. Initially, the concentration increases because of the high diffusional fluxes. With the passage of time, as the film rises in the film section it faces an increasingly stronger light intensity and hence encounters a faster photochemical reaction kinetics. Consequently, the concentration of *A* in the bulk of the film starts decreases beyond a certain time of contact in the film section.

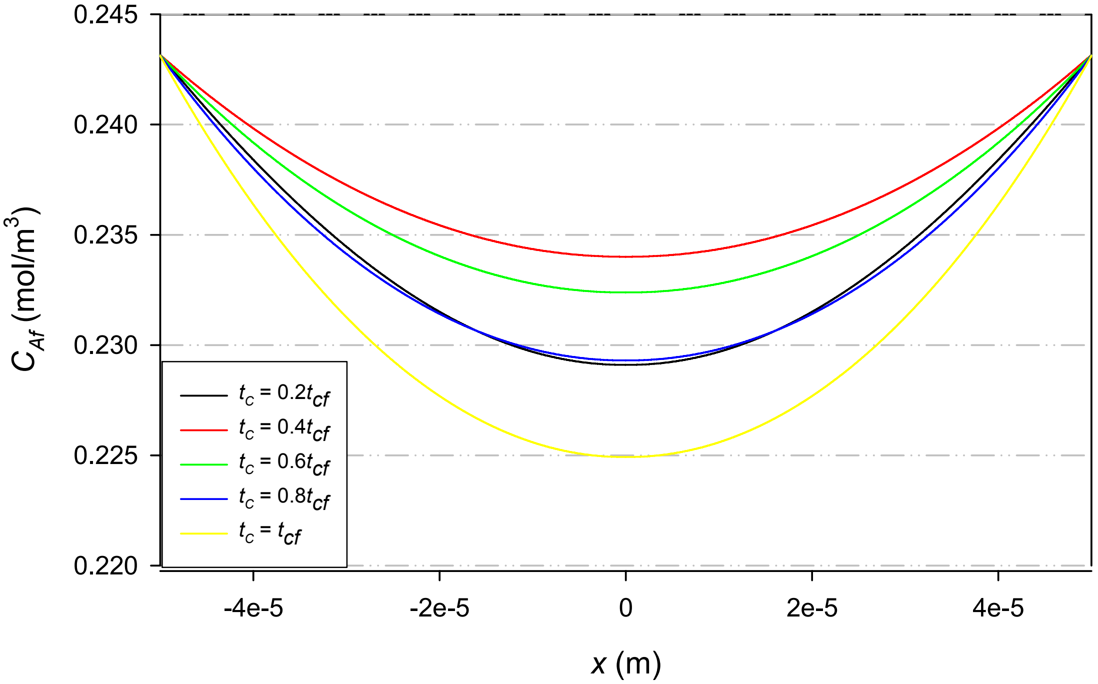

Figure-3, Transient concentration profile in film, in presence of light ($I_O = 10^{-3}$ E/(m^{2}·s), $K_2 = 10^{-5}$, $Q_1 = 0$ m3/s)

Effect of Light Intensity and Dark-Reaction Rate Constant

Figures 4 and 5 illustrate the effect of light intensity on the absolute performance of the film reactor and that relative to a bubble column reactor respectively. Figure 4 presents the transient fractional reaction rate in the film section, Γ. It is seen that the fractional rate in the film section is close to 2 percent in absence of light which reaches to as high as 49% for an incident intensity light intensity of 10^{-2} E/(m^2.s). Thus with a typically strong light intensity, as much as 49% of the reaction is completed in just 1.7 percent of the total reactor volume. Figure 5 shows how the ratio of rate of reaction in the film reactor to that in a bubble-column reactor, X, varies with time for different incident-light intensities. It increases with an increase in the light intensity, e.g. for a light intensity of 10^{-2} E/m^2/s, the rate in a photochemical-film reactor is almost twice that in a bubble column reactor. Thus for conducting photochemical gas-liquid reactions, a film reactor may be a more attractive option than a bubble- column reactor.

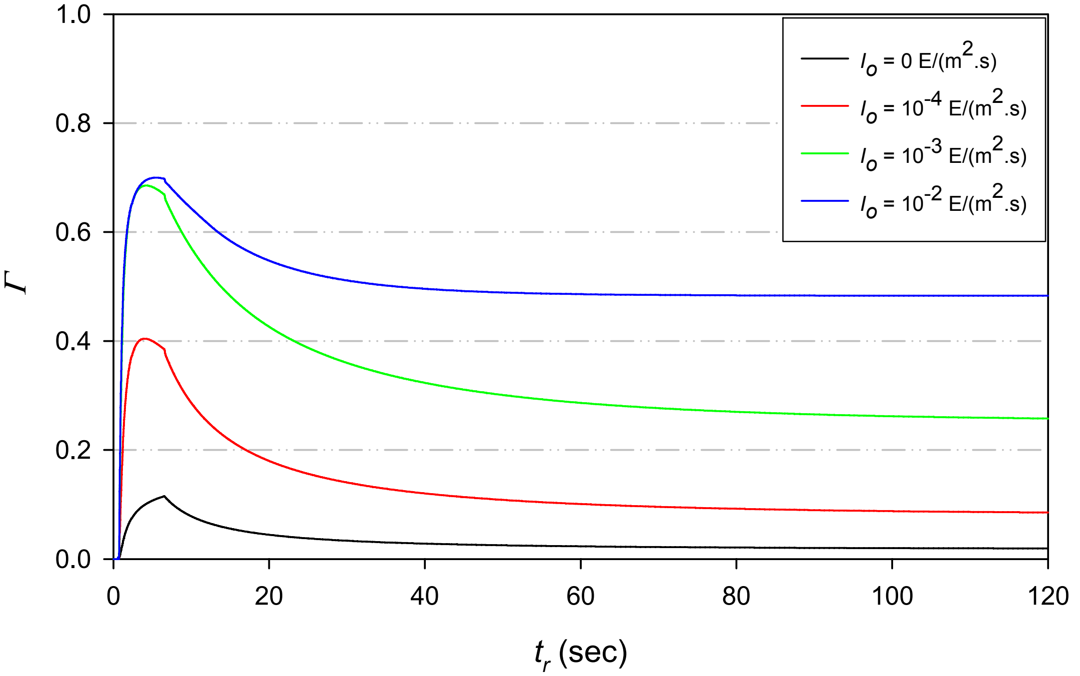

Figure-4, Γ vs time for different I_o, (K_2 = 10^{-5} m^3/(mol.s), Q_1 = 0 m^3/s)

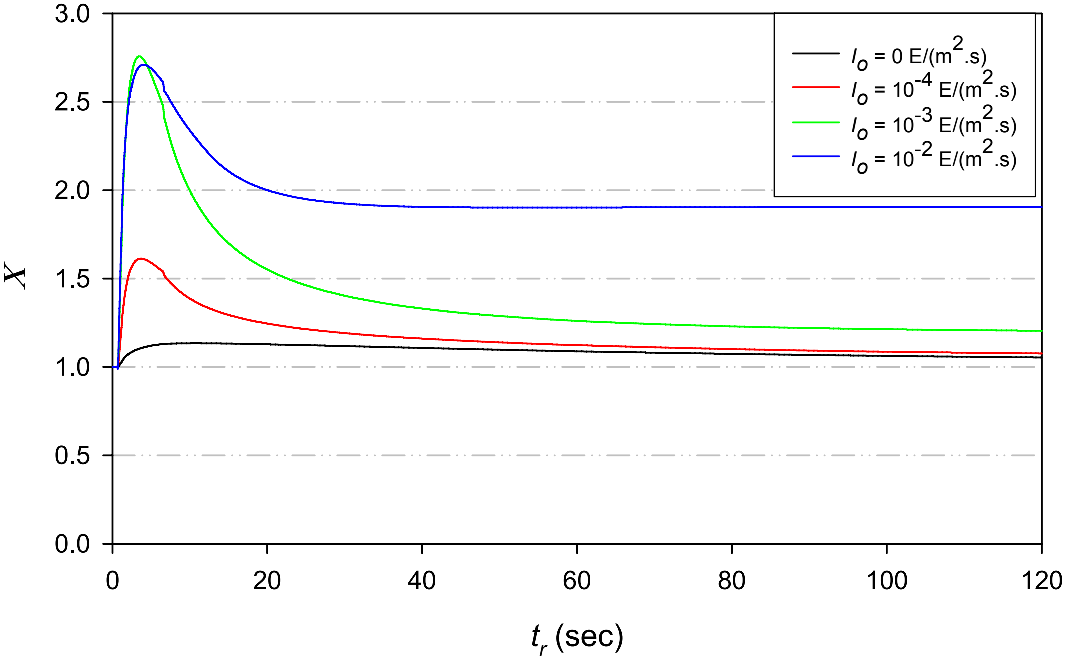

Figure-5, X vs time for different *Io*, (K_2 = 10^{-4} m^3/(mol.s), Q_1 = 0 m^3/s)

Figure 6 shows the variation of fractional rate of reaction in the film section, Γ, with time for three different dark-reaction rate constant values in absence of light. The fractional rate in the film section increases initially with time and with increase in the rate constant. It shows eventually a maximum with time. The enhancement in the film section increases as the reaction-rate is increased (either through the photochemical or through the dark route). the diffusional resistance starts playing an increasingly important role. Under these conditions, the fractional rate of reaction in the film section increases because of much smaller diffusional length scales provided by the liquid film.

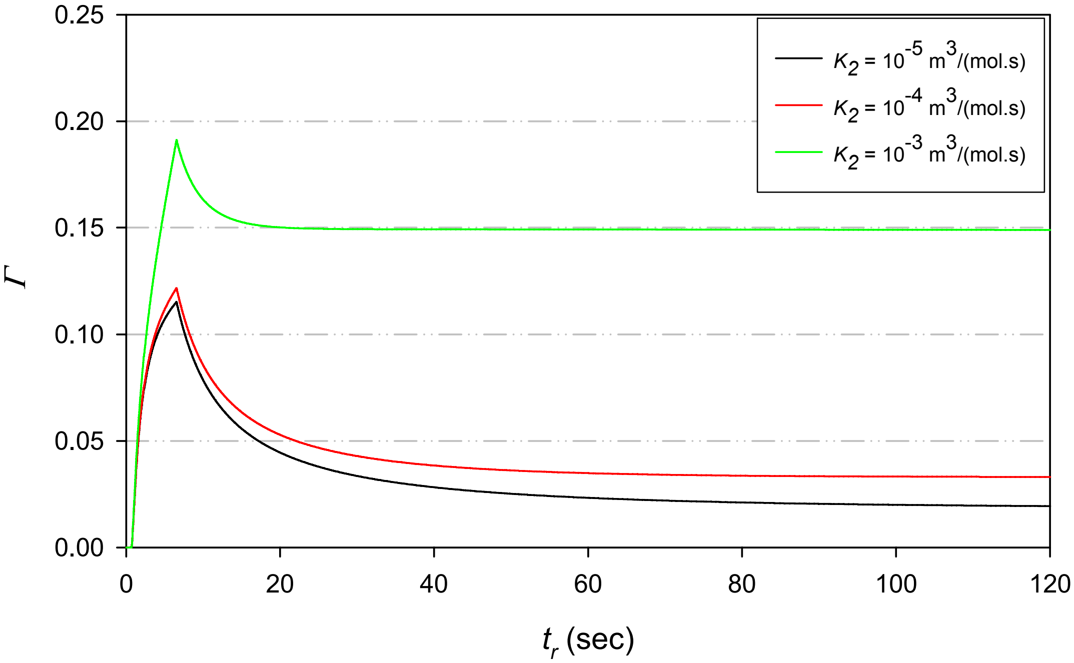

Figure-6, Γ vs time for different K_2, (I_o = 0 E/(m^2.s), Q_1 = 0 m^3/s)

Effect of Liquid Cross Flow Rate

Figure 7 shows the transient fractional rate of reaction in the film section for different liquid cross-flow rates. With the increase in cross-flow rate there is a slight increase in Γ. The storage liquid rich in dissolved gas-phase A is replaced by fresh cross flow liquid free of A, thus decreasing the concentration C_A. This decreases the rate of reaction in the storage section and hence results in an increase in Γ.

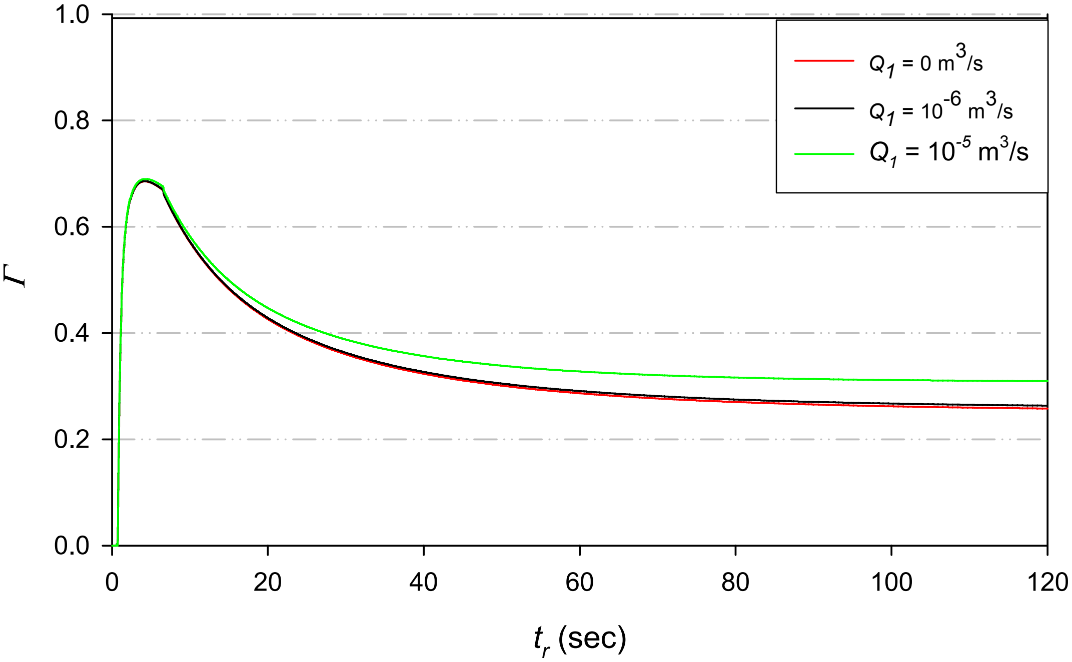

Figure-7, Γ vs time for different Q_1, ($I_O = 10^{-3}$ E/(m^2.s), $K_2 = 10^{-5}$ m^3/(mol.s))

Effect of Height of Film Section

The ratios of rate of reaction in the film reactor to that in a bubble-column reactor for different heights of the film section have been shown in figure 8 for very slow dark reaction ($K_2 = 10^{-7}$ m^3/(mol.s). It is seen that for small reactor (height <= 100 cm), this ratio increases with increase in height. An increase in the height means more liquid in the film section and hence greater extent of reaction.

But for reactors with heights of about 100 cm-200 cm the values of X are nearly same. In other words, after a critical height there is very little effect of the increase in the height of film section. The films at the top of the reactor of about a meter screen the light and limit reaching the bottom, and hence there is negligible extent of reaction actually occurring in the bottom portion of the film section This explains the limiting envelope seen in the transient relative performance of a film reactor, with respect to height of film section, when compared to bench mark of a bubble column reactor.

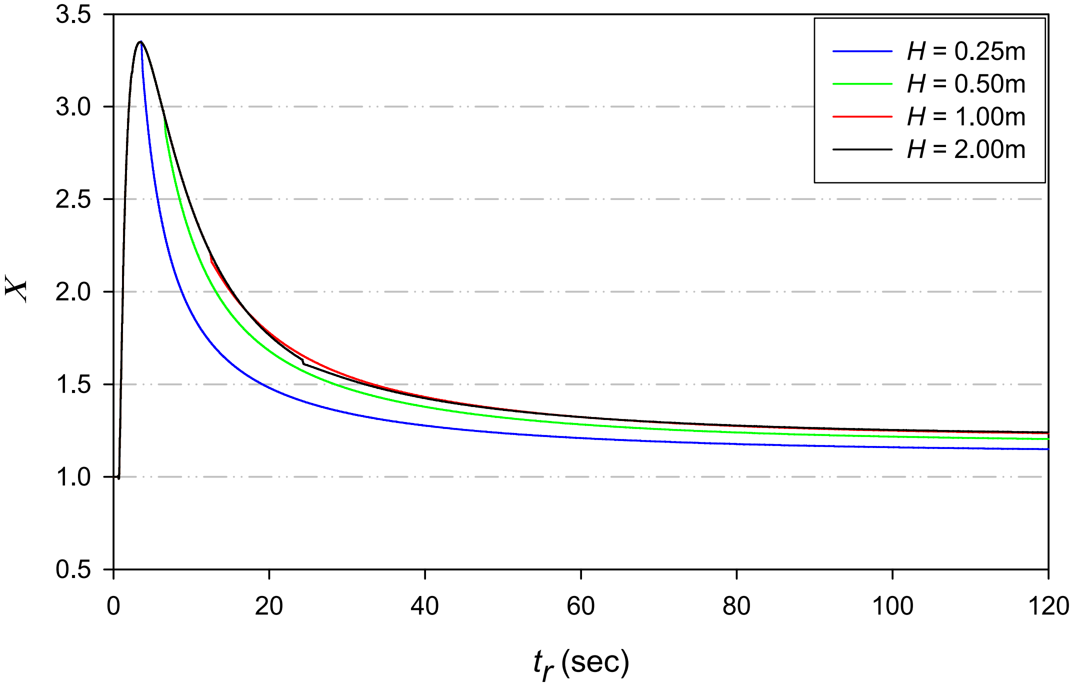

Figure-8, X vs time for different heights of film section
($I_o = 10^{-3}$ E/(m^2.s), $K_2 = 10^{-7}$ m^3/(mol.s), $Q_1 = 0$ m^3/s)

CONCLUSIONS

In this study, a novel photochemical film reactor for fast gas-liquid photochemical reactions has been proposed. It has been found that the parallel-film photochemical reactor gives better conversion as compared to a bubble-column photochemical reactor. The utility of parallel film photochemical film reactor improves with increase in reaction kinetics. It also revealed that with large excess of liquid phase reactant highest conversions are achieved for semi-batch mode of operation (batch with respect to liquid-phase). On studying the effect of height of film section it has been found that the reactor performance increases up to a critical height after which there is negligible effect of increasing film section height. In this paper we have not analyzed the effect of multiple reflections in the film section, as we have considered no reflection at gas liquid interface. But in any real reactor there will be multiple reflections in the film section and hence film reactor will give an even better performance.

NOMENCLATURE

a	thickness of half film, m
A	gas-phase reactant
b	stoichiometric factor (moles of B or B* reacted per mole of A), dimensionless
B	liquid-phase reactant
C_A	concentration of A in the liquid in the storage section, mol.m^{-3}
$C_A^{'}$	concentration of A, dissolved and free in the surface elements near the gas-liquid interface in storage section, mol.m^{-3}
C_{Af}	concentration of A at coordinate position x and time t_c in film, mol.m^{-3}
C_{AF}	concentration of A in drainage from film section, mol.m^{-3}
C_{Ag}	concentration of A in gas phase in storage section, mol.m^{-3}
C_{AG}	concentration of A in gas pocket, mol.m^{-3}
C_{Agi}	concentration of A in gas phase entering the storage section, mol.m^{-3}
C_{Ao}	concentration of A in cross flow liquid entering the storage section, mol.m^{-3}
C_A^*	concentration of A in liquid in equilibrium with the gas in storage section when the film or element is formed, mol.m^{-3}
C_B	concentration of B in the liquid in storage section, mol.m^{-3}
C_{Bo}	concentration of B in cross flow liquid entering the storage section, mol.m^{-3}
D_A	diffusion coefficient of A in liquid, m^{2}s^{-1}
g	acceleration due to gravity, ms^{-2}
h	height of the storage section, m
H	height of the film section, m
I_a	intensity of light absorbed in the film section, E.m^{-2}s^{-1}
I_i	intensity of light falling at a film, E.m^{-2}s^{-1}
I_o	initial intensity of light, E.m^{-2}s^{-1}
I_{on}	intensity of light after passing through ‘n_f’ films, E.m^{-2}s^{-1}
$I_o^{'}$	local intensity of light in storage section, E.m^{-2}s^{-1}
I_o^s	intensity of light at top of the storage section, E.m^{-2}s^{-1}
I_r	intensity of light reflected by a film, E.m^{-2}s^{-1}
I_t	intensity of light transmitted by a film, E.m^{-2}s^{-1}
k	wave number of radiation, m^{-1}
K_2	second-order rate constant for dark reaction, m^{-3}.mol^{-1}s^{-1}
$K_2^{'}$	quantum yield, mol/E
K_e	equilibrium distribution coefficient for A at the gas-liquid interface, dimensionless
l	path length of light in storage section, m
M_{fr}	total amount of free A in a half film, mol
M_r	amount of A reacted in a half film, mol
M_t	total amount of A diffused into a half film, mol
n	reflective index of liquid, dimensionless
n_f	number of films above a given film, dimensionless
N_b	number of bubbles in the storage section, dimensionless
N_t	number of tubes in the film section, dimensionless
Q_1	flow rate of liquid across the storage section, m^3.s^{-1}
Q_f	drainage-flow rate of liquid from film section to storage section, m^3.s^{-1}

Q_t	total volumetric flow rate of gas, m^3s^{-1}
R_b	radius of a bubble, m
r_f	overall rate of reaction in film section, mol/s
R_t	radius of a tube in film section, m
R_s	overall rate of reaction in storage section, mol/s
S	surface area of a film, m^2
t	time of bubble rise in storage, s
t_c	time of a liquid-film rise in film section, s
t_{cd}	residence time of a bubble in storage section, s
t_{cf}	residence time of a film in film section, s
t_d	life time of a surface element in storage section, s
t_e	time spent by a surface element at gas-liquid interface, s
t_r	time of reactor operation, s
u_b	bubble-rise velocity in film section, $m.s^{-1}$
u_{bs}	bubble-rise velocity in storage section, $m.s^{-1}$
u_g	superficial gas velocity in storage section, $m.s^{-1}$
u_t	terminal velocity of a single gas bubble in storage section, $m.s^{-1}$
V_L	volume of liquid in the gas-liquid dispersion in the storage section, m^3
V_1	volume of a liquid film, m^3
V'	volume of gas in the storage section, m^3
V_p	volume of half gas pocket, m^3
x	position coordinate in a liquid film with origin placed at the center, m
x_e	position coordinate in a surface element with origin placed at the interface, m

Greek letters

α	extinction coefficient for liquid, $m^2.mol^{-1}$
α'	effective extinction coefficient for film section, $m^2.mol^{-1}$
β	variable defined in condition (vi), s^{-1}
Γ	transient fractional rate of reaction in the film section, dimensionless
δ_f	thickness of a liquid film, m
δ_p	thickness of a gas pocket, m
ε	gas hold-up in storage section, dimensionless
λ	pseudo-first order rate constant for dark reaction, s^{-1}
ρ	fraction of amplitude of electric field reflected at gas liquid interface
ρ_l	density of liquid, $kg.m^{-3}$
σ	surface tension of liquid, $N.m^{-1}$
τ	fraction of amplitude of electric field transmitted at gas liquid interface
X	ratio of rate of reaction in the film reactor to that in the bubble-column reactor

REFERENCES

1) Bhaskarwar, A.N., and R. Kumar, “Analysis of a Photochemical Film Reactor,” *AIChE J.* **37** (3), 475 (1991).
2) Bhaskarwar, A.N., and R. Kumar, “ General Model of a Foam Bed Reactor,” *Chem. Engg, Sci.* **45** (5), 1155 (1990).
3) Deckwer, W.D., *Bubble Column Reactor*, John Wieley & Sons, 190 91992).
4) Fisher, M., “Photochemical Syntheses on the Technical scale,” *Angew. Chem.*, **90,** 17 (1978).
5) Mahajani, V.V., and M.M. Sharma, “ Gas Absorption With Photochemical Reaction,” *Chem. Engg. Sci.* **36**(3), 595 (1981).
6) Marrucci G., 1964, I&E C Fundamentals, Page224.
7) Prengle, Jr., H.W., C.E. Mauk, R. W. Legan, and C.G. Hewes, “Ozone/UV Process Effective Waste Water Treatment.” *Hydroc. Processes*, **54**, 82 (1975).
8) Schorr, V., B. Boval, V. Hancil, and J.M. Smith, “Photooxidation Kinetics of Organic Pollutants in Munucupal Waste Water,” *Ind. Eng. Chem. Process Des. Dev.*, **10**, 509 (1971)
9) Zhao, W., Z Wu, H Shi and D Wang, “UV Photodegradation of Azo dye Diacryl Red X-GRL”, *J. Photochem. Photobio. A, Chem.*, **171** (2), 97 (2005)